PHILOSOPHICAL TRANSACTIONS OF THE ROYAL SOCIETY A MATHEMATICAL, PHYSICAL & ENGINEERING SCIENCES

Satellite-Borne Measurements of the Composition of the Middle Atmosphere

F. W. Taylor, A. Dudhia and J. G. Anderson

Phil. Trans. R. Soc. Lond. A 1987 **323**, 567-576
doi: 10.1098/rsta.1987.0105

Phil. Trans. R. Soc. Lond. A **323**, 567–576 (1987)
Printed in Great Britain

Satellite-borne measurements of the composition of the middle atmosphere

By F. W. Taylor and A. Dudhia

Department of Atmospheric Physics, Clarendon Laboratory, University of Oxford, Parks Road, Oxford OX1 3PU, U.K.

[Plates 1 and 2]

Atmospheric dynamics and photochemistry can be studied by using measurements of temperature and composition made by remote sensing from satellites. This paper describes the pressure-modulation technique, which is employed by the stratospheric and mesospheric sounder (SAMS) experiment on the satellite *Nimbus* 7, and by an advanced version (the improved stratospheric and mesospheric sounder or ISAMS) now under construction for the forthcoming Upper Atmosphere Research Satellite programme. SAMS measurements of methane and nitrous oxide for the three-year period from 1 January 1979 to 31 December 1981 are presented, and show the latitudinal and seasonal variability of the average concentration of these long-lived minor constituents. From the observed behaviour, some aspects of the circulation of the middle atmosphere are identified and their possible origins discussed.

Introduction

The study of stratospheric minor constituents is interesting for three main reasons. The first of these is the desire to understand photochemical processes in the region, particularly those involving water vapour and ozone, two species of crucial importance to the fragile terrestrial biosphere. The second is the belief that certain of the longer-lived species can be used as tracers of the motions and that therefore, in conjunction with temperature measurements, they may be used to investigate the dynamical behaviour of the middle atmosphere, which at present is quite poorly understood. Finally, there is the prospect of discovering more about the nature and extent of the principal sources and sinks of minor constituents, in particular of understanding the relative importances of manmade against natural sources, and the regulatory mechanisms that act, or could be brought into play, when harmful changes begin, for whatever reason, to occur.

The background physics to these problems has been discussed by many authors. For a recent introduction aimed at undergraduate-level physicists, see Taylor (1987). Advanced theory requires the use of computer models of the atmosphere, with detailed parameterizations of its structure, dynamics and photochemistry; some of these are discussed by Pyle *et al.* (this symposium). The present paper is concerned mainly with measurements, particularly those made from satellites. Satellite measurements are particularly powerful because they afford continuous, global coverage, which is often essential to unravelling the complex processes at work.

The SAMS and ISAMS experiments

The stratospheric and mesospheric sounder (SAMS) is an example of the current generation of advanced instruments that has produced global data on some of the more interesting minor constituents. Of these, we shall concentrate on methane (CH_4) and nitrous oxide (N_2O), because the data for these from SAMS is the most completely analysed and the conclusions that we are able to draw are the most mature. N_2O and CH_4 are both important minor constituents of the stratosphere for several reasons. Neither gas has a known photochemical source in the middle atmosphere, both originating near the surface by a variety of processes that includes anthropogenic sources in each case (see Wayne 1985). As both gases have fairly long lifetimes against photochemical destruction (ranging from about a year for methane in the lower stratosphere to a few weeks for nitrous oxide near the stratopause), they are important tracers of the transfer process across the tropopause and of the stratospheric mean circulation. Methane is a source of water vapour in the middle atmosphere as a result of a series of reactions equivalent to

$$CH_4 + 2O_2 = CO_2 + 2H_2O,$$

whereas nitrous oxide is the main source of stratospheric NO_x by a series equivalent to

$$2N_2O + O_2 = 4NO.$$

SAMS was also designed to measure nitric oxide, NO, but because of a technical problem these measurements were of poor quality. It also had channels that obtained much valuable data on stratospheric and mesospheric water vapour and carbon monoxide; these are reported elsewhere (Drummond & Mutlow 1981; Barnett *et al.* 1985; Murphy 1985). It also, of course, like its predecessors on *Nimbus* 4, 5, and 6, made measurements of temperature (Barnett, this symposium). The ISAMS is intended to repeat the SAMS measurements with significantly better global coverage, much higher sensitivity, and additional species including other members of the nitrogen-oxide family (table 1).

Measurement technique and instrumentation

The stratospheric and mesospheric sounder is a nine-channel, limb-viewing infrared radiometer employing the pressure-modulation technique (Taylor 1983) to observe thermal emission from carbon dioxide (for temperature retrievals) and five other atmospheric minor constituents. The instrument itself has been described by Drummond *et al.* (1979). The principles upon which it operated are basically the same as its much more advanced successor ISAMS, which is described below.

The improved stratospheric and mesospheric sounder is being built for the Upper Atmosphere Research Satellite, the first of a new generation of modern spacecraft for atmospheric research. (The *Nimbus* design, which dates back to about 1960, became obsolete after *Nimbus* 7 was launched in 1978.) A full technical description of the ISAMS instrument is beyond the scope of the present paper, but the following outline is given to permit an appreciation of the principles from which the scientific data is obtained, and the improvements over SAMS which have been incorporated in the new instrument. The latter are summarized in table 1.

Figure 1 shows a schematic diagram of a single channel of the ISAMS. Like SAMS, the instrument

PHILOSOPHICAL TRANSACTIONS OF THE ROYAL SOCIETY A MATHEMATICAL, PHYSICAL & ENGINEERING SCIENCES

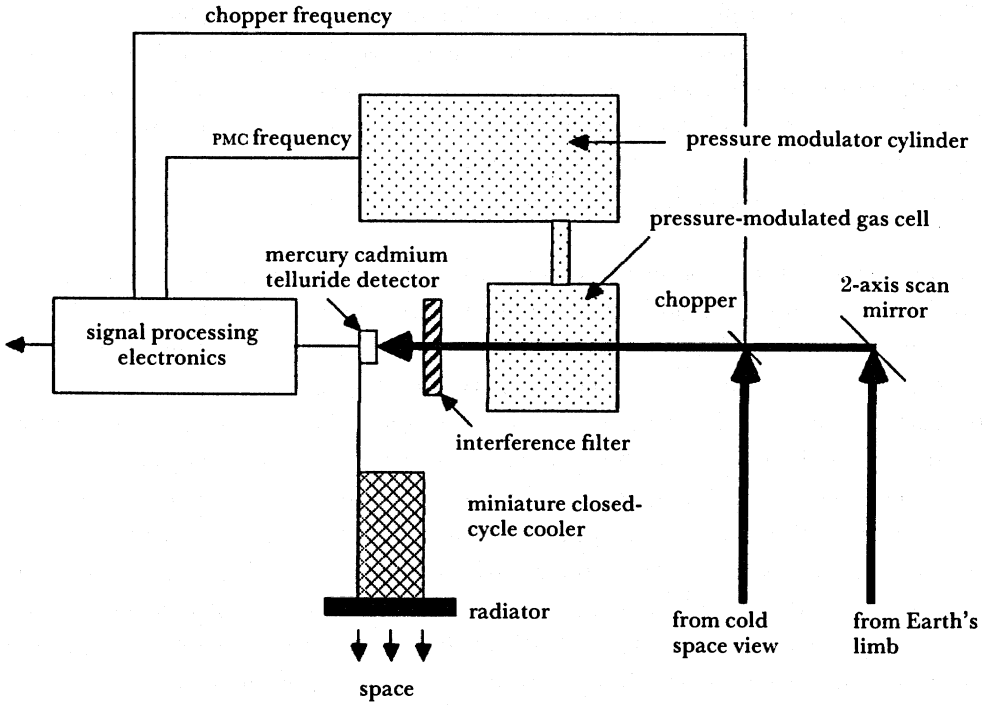

FIGURE 1. Schematic diagram of a single channel of the ISAMS.

TABLE 1. COMPARISONS BETWEEN SAMS AND ISAMS

	SAMS	ISAMS
vertical resolution	10 km	2.4 km
integration time (typical, for a signal to noise ratio of 100:1)	20 s	2 s
number of detectors	6	32
species observed	CO_2, H_2O, CH_4, CO, N_2O, NO	CO_2, H_2O, CH_4, CO, N_2O, NO, NO_2, N_2O_5, HNO_3, window
latitude coverage	50° S–70° N	80° S–80° N

views sideways from the spacecraft, that is, at a tangent to the Earth's surface, to observe the atmosphere at the limb. Thermally emitted radiation from the atmosphere is collected by the main telescope mirror and focused onto the rotating blade of a mechanical chopper which modulates the beam at a frequency of 1 kHz. The chopper has a reflecting face, so that the amplitude of the modulated beam is referred always to the zero radiance level from cold space, which is viewed through a port on the side of the instrument.

After mechanical chopping, the beam is modulated for a second time by a pressure-modulator cell (PMC); this contains gas at a pressure of typically 1–20 mbar†. In the PMC, modulation of the infrared beam is achieved by a cyclic variation of the pressure in the cell using a resonant piston arrangement. The near-sinusoidal variation in the mean cell pressure results in a corresponding variation in the amount of absorption that occurs during the passage of the beam through the gas in the cell, thus modulating the radiation in the spectral lines of

† 1 mbar = 10^2 Pa.

the gas of interest (Taylor 1983). Because the lines of all other atmospheric species than the one contained in the cell are absent, the radiation is selectively labelled by this technique.

To make the eventual data analysis easier, another, coarser, stage of spectral selection is included after the PMC to restrict the radiation reaching the detector to a small part of one of the strong vibration–rotation bands of the species observed. This component is a specially developed multilayer interference filter, typically 20 or 30 wavenumbers wide (Seeley *et al.* 1981).

Finally, the signal is synchronously demodulated at the two frequencies (i.e., those of the chopper and the PMC) simultaneously, to give two independent signals. The 'wide-band' signal (that at the chopper frequency) is a measure of the radiance in the relatively wide spectral band defined by the interference filter. In this respect ISAMS performs like a conventional radiometer, similar to LIMS (Russell & McCormick, this symposium). The signal at the other frequency originates in or near the centres of the spectral lines of the species in the modulator cell, and is therefore very selective of that species and rejects all others except when the lines actually overlap. The principal reason for acquiring both is the fact that the wide-band signal is available to deeper levels in the atmosphere, where the spectral line centres are completely absorbing, so the total vertical coverage is extended thereby. It is also more sensitive to continuum absorbers such as aerosol; comparisons between retrievals from the wide-band and the pressure-modulated channels while looking at the same region of the atmosphere are a useful check that the signal is not excessively contaminated by, for example, ice clouds or volcanic effluent.

The single channel of ISAMS represented in figure 1 is one of eight in the instrument as a whole. Figure 2 shows the overall layout. Pressure modulators containing the following gases are included: CO_2 (two), CO, CH_4, NO, N_2O, NO_2, and H_2O. The reason for having two CO_2 modulators is to be able to work with two mean cell pressures simultaneously. This assures good temperature profiling over a wide range, and also allows the determination of pressure at a reference altitude where the coverage of the two overlaps (Rodgers *et al.* 1984). The CO_2 channels contain four-position filter wheels (figure 2); these allow wide-band measurements to be obtained from time to time of three key species that cannot be contained in modulator cells, that is, ozone, nitric acid (HNO_3) and dinitrogen pentoxide (N_2O_5). The other filter positions select different parts of the CO_2 band near 15 μm, and are for optimising the temperature profile determination. Temperature is a fundamental atmospheric structure variable and is also a prerequisite for retrieving composition; ISAMS is the principal temperature sounding instrument on *UARS*.

Each of the infrared detectors shown in figure 2 is actually a small array of four independent elements each 1.05×0.15 mm^2 in area. Four 'slabs' of atmosphere are thereby measured simultaneously; this multiplexing allows the whole atmosphere from the tropopause to the mesopause to be scanned every 16 s, with a vertical resolution of 2.4 km. The horizontal resolution along the sub-spacecraft track is determined by the orbital motion that takes place in that time, and is rather more than 100 km. The horizontal resolution in the perpendicular dimension is determined both by the contribution function for radiation emitted along the line of sight and by the spacing between successive orbits. From calculations the former is about 200 km, whereas the latter varies with latitude from 0 to *ca.* 1500 km.

PHILOSOPHICAL TRANSACTIONS OF THE ROYAL SOCIETY A MATHEMATICAL, PHYSICAL & ENGINEERING SCIENCES

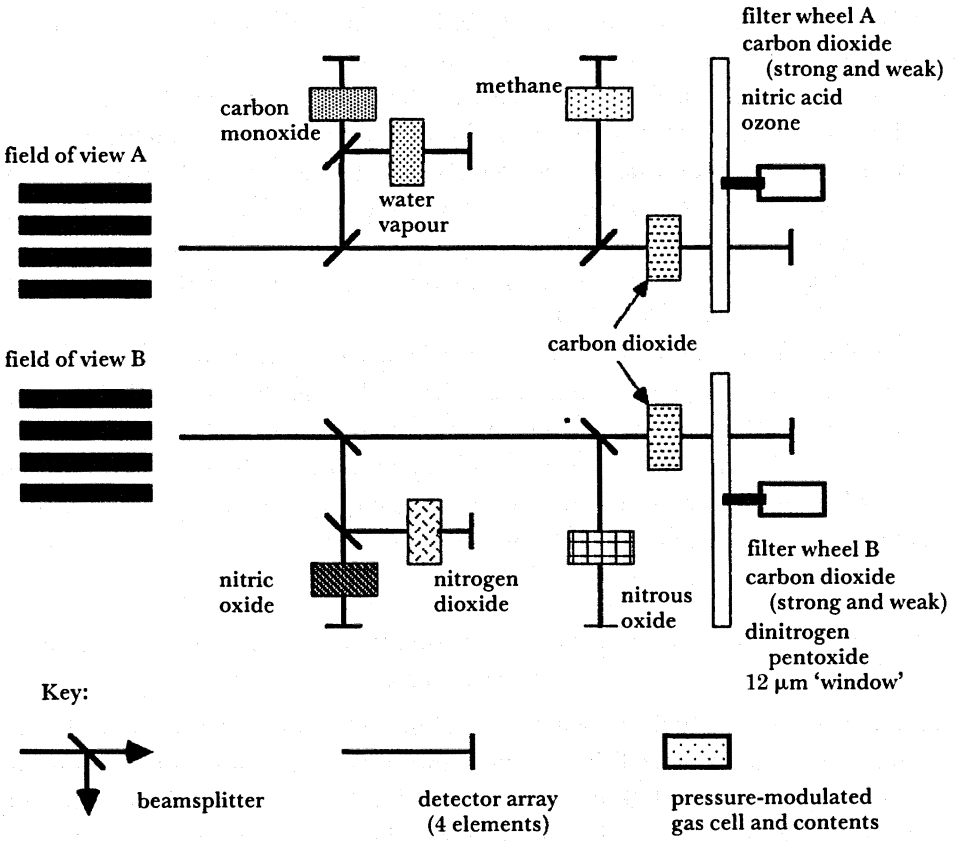

FIGURE 2. Block diagram of the ISAMS.

SAMS OBSERVATIONS OF METHANE AND NITROUS OXIDE

On board the *Nimbus* 7 spacecraft in polar, sun-synchronous orbit, SAMS made observations from October 1978 to June 1983. Methane was measured in the ν_4 band centred near 7.6 μm and nitrous oxide in the ν_1 band centred near 7.8 μm. Both channels shared the same pyroelectric detector and the instrument had a 75% duty cycle; hence the observations of either species occupied about one-third of each month on average. The vertical resolution of the measurements is about 10 km.

Earlier discussions of the methane and nitrous oxide observations, including the retrieval of abundances from radiance observations and an analysis of the error budget, can be found in the papers by Jones & Pyle (1984), Jones (1984) and Rodgers *et al.* (1984). Profiles were actually retrieved at seven altitudes, including a fixed base value at 1.4 scale heights (250 mbar). The other levels were 2.6, 3.8, 5.0, 6.2, 7.4, and 8.6 scale heights (75, 20, 7, 2, 0.6, and 0.2 mbar respectively). Most of the useful information, however, is restricted to levels between 20 mbar at the lower end of the range and 0.2 (for CH_4) or 0.6 mbar (for N_2O) at the top.

The SAMS N_2O and CH_4 observations are not entirely independent, because their spectral bands overlap, and data from one species is required by the retrieval program to determine the other. Vertical correlations are introduced by the finite field of view of the instrument and temporal correlations by the 'sequential maximum likelihood operator' approach used for the retrieval (Rodgers *et al.* 1984). There is also some latitudinal interdependence in the data,

introduced by the temperature retrieval algorithm. All of these effects are small, however, especially in monthly averages like those used here.

The accuracy of the retrieved zonal mean as determined by Jones & Pyle (1984), who combined conservative estimates of all of the known sources of error including spectroscopic and retrieval uncertainties, and noise due to instrumental sources and spacecraft jitter, varies with height but is at best 20% for CH_4 and 25% for N_2O. The corresponding precision is *ca.* 3% for CH_4 and *ca.* 6% for N_2O. The 'confidence limits' established by the same authors for the vertical range of the measurements is 20 mbar (*ca.* 25 km) to 0.2 mbar (*ca.* 60 km) for CH_4 and 0.6 mbar (*ca.* 53 km) for N_2O.

Comparisons have been made between SAMS retrievals and other measurements, particularly from balloons (Jones & Pyle 1984; Taylor *et al.* 1986). The *in situ* and satellite data agree quite well near the top of the region of overlap (about 10 mbar or 30 km), but lower down discrepancies occur with the SAMS amounts being systematically higher. The reason for this is still being investigated. In the present paper we will concentrate on looking for latitudinal and seasonal trends, so the difference is probably unimportant.

The distribution and variability of methane and nitrous oxide in the stratosphere

Satellite experiments produce such a large volume of data that interpretation becomes a matter of producing maps of carefully selected and averaged quantities. For the purposes of producing the maps in figures 3–6, plates 1 and 2, the data was smoothed with a filter based on a logarithmic (mixing ratio) grid of 5 altitudes × 12 latitudes × 14 months (i.e. replicating January and December at each end to ensure continuity in time). Each grid point was then combined with a value obtained from the interpolation of up to 13 pairs of adjacent grid points, each reduced to 10% weighting. This gives a relatively small amount of smoothing, which removed a few 'rogue' points and smoothed out the sharper features that, although real, were probably atypical.

Maps were produced by averaging the SAMS data for the three-year period from January 1979 to December 1981 and applying some smoothing. As noted above, SAMS actually made observations from shortly after launch on 24 October 1978 until June 1983, but the early data consist mainly of instrument checkout modes whereas those obtained after March 1982 were rendered more difficult to interpret by the volcanic dust injected into the stratosphere by the eruption of the volcano El Chichon, and will require further validation.

Averages were formed first by day and by latitude, the latter in 10° bins. The daily data and their estimated errors were then used to produce an error-weighted average by month, before the corresponding months for the three years were combined. Thereafter, the 'error' was taken to be the square root of the greater of either the variance or the inverse sum of the weights of

---

Description of plate 1

Figure 3. Monthly mean abundances of methane in parts per million by volume as measured by SAMS. The ordinate is logarithmic pressure from 20 to 0.2 mbar (approximately 20–60 km), and the abscissa is latitude. The data are zonal averages in 10° latitude bins for the three years 1979–81.

Figure 4. Deviations from the three-year (1979–81 inclusive) annual mean mixing ratio of methane, expressed in percentages as a function of altitude (pressure) and latitude, for each month of the year.

3

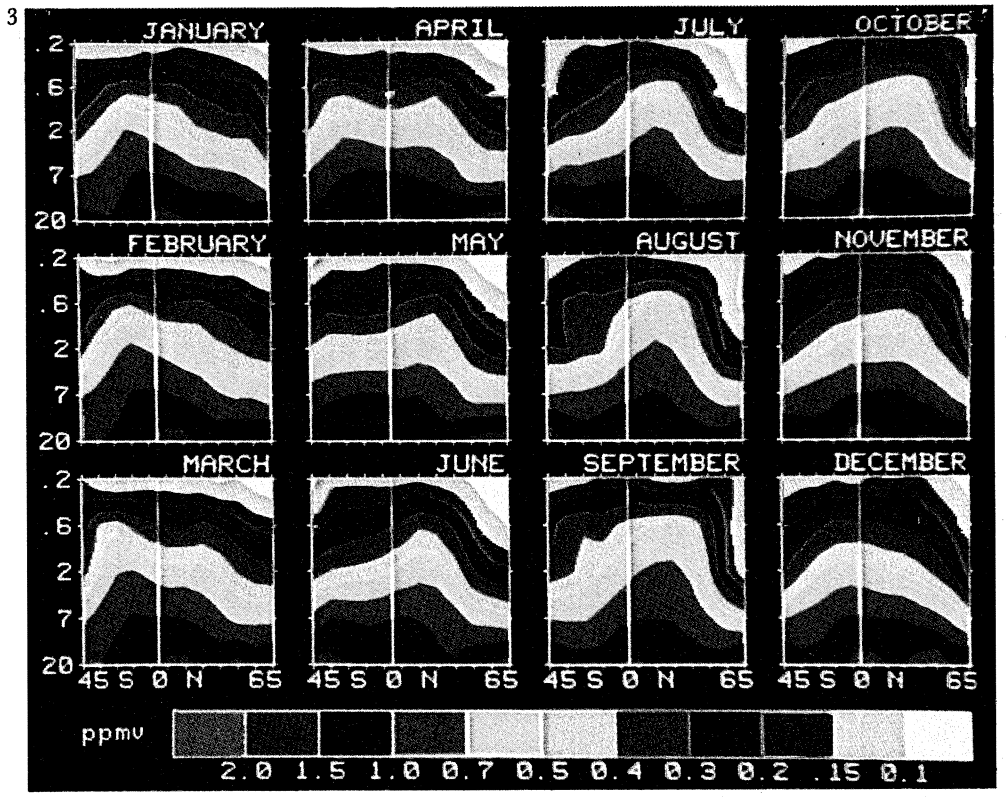

4

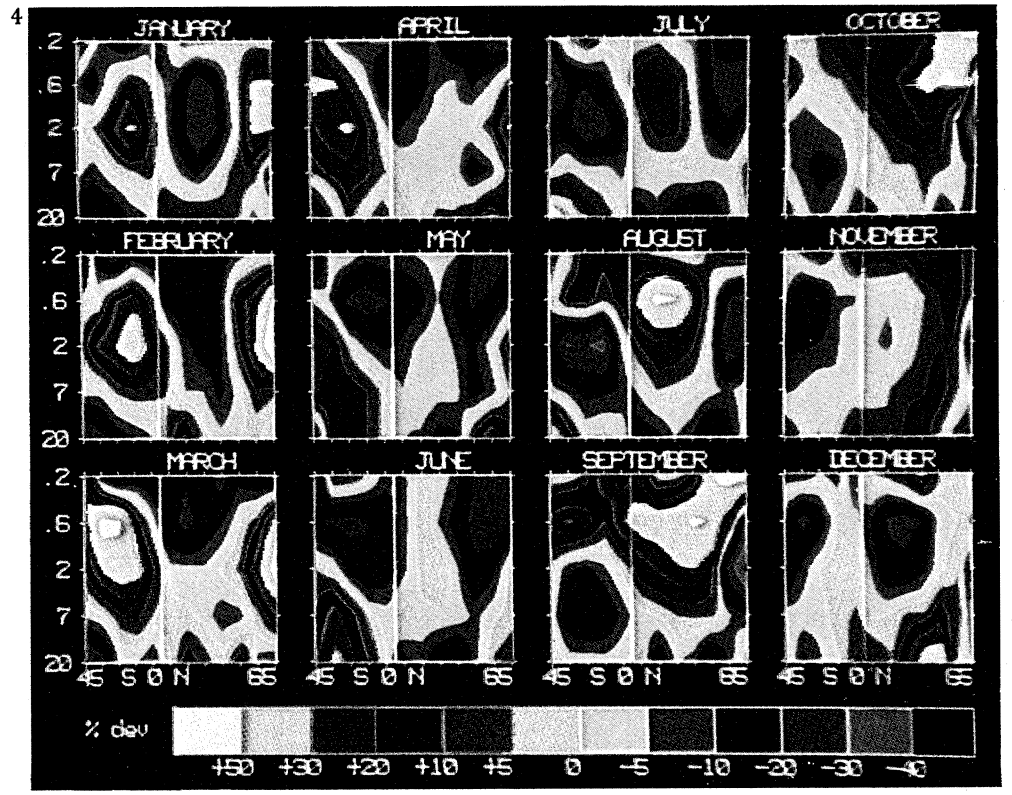

FIGURES 3 AND 4. For description see opposite.

5

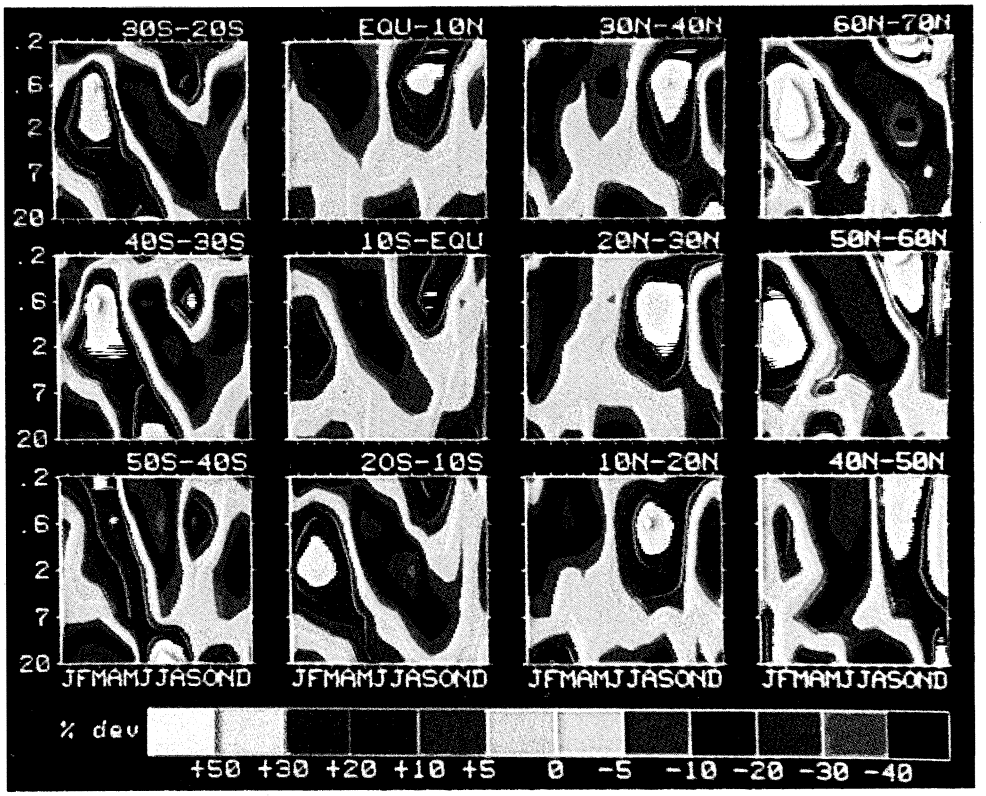

6

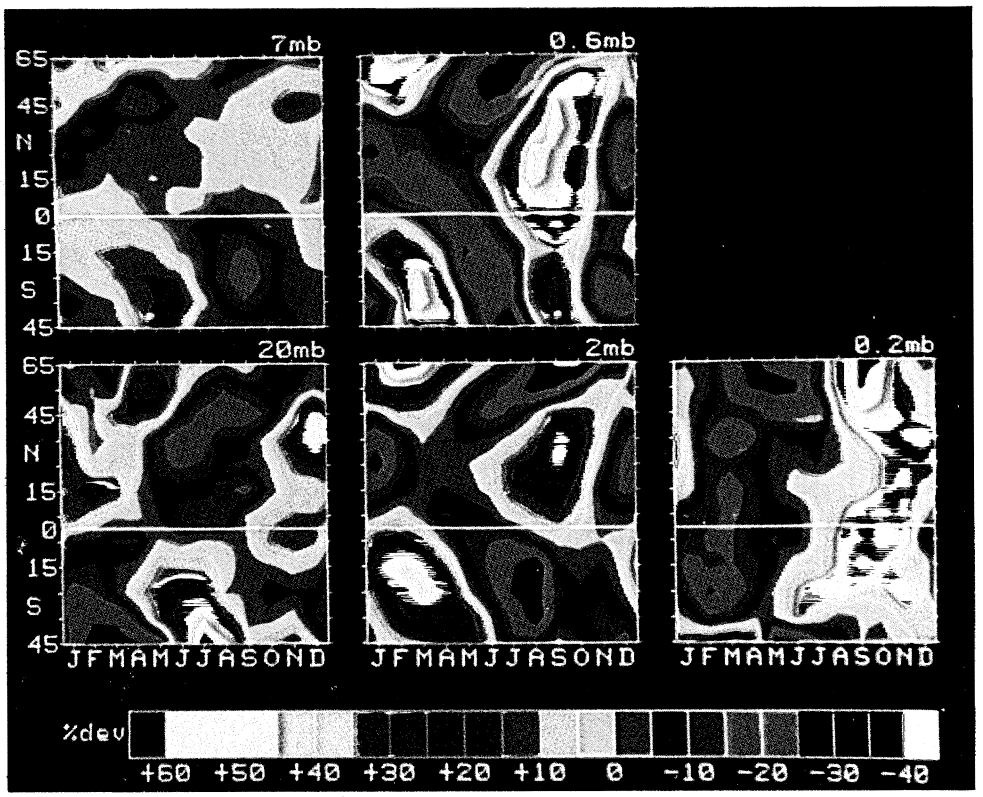

FIGURES 5 AND 6. For description see opposite.

the contributing data. This approach brings in the standard deviation of the profiles contributing to the mean.

Figure 3, plate 1, shows maps from SAMS data of the zonal mean methane abundance as a function of latitude, for each month of the year. In figures 4–6, plates 1 and 2, the three-year average for all seasons has been subtracted, to emphasize seasonal variations and their latitude and height dependence. The same data set is plotted in three different ways in figures 4–6 so that the various features can be seen most distinctly.

When the data are presented as deviations from the mean, the overall appearance of plots for either CH_4 or N_2O is quite similar. This in itself is a significant result, suggesting that the distribution is controlled more by dynamics than chemistry. This, of course, is not unexpected, because both species are believed to have long lifetimes against photochemical destruction in the stratosphere (see, for example, Solomon *et al.* 1986). Plots for methane only are presented for conciseness, but except where otherwise stated the major features to be described are generally seen in maps of both species.

Plots similar to figure 3 have been described and discussed by Jones & Pyle (1984), Jones (1984), Holton (1986), Gray & Pyle (1986), Solomon *et al.* (1986), and several other authors. They all noted the general characteristics of the distribution, which features negative gradients with latitude and with height, so that the general appearance is of a bulge over low latitudes. Following the monthly changes, the most noticeable trend is for the bulge to migrate towards the summer hemisphere. This is because of the seasonal dependence of the mean circulation, a feature of which must be more rapid vertical transport in the summer than in the winter. The total amounts of methane and nitrous oxide, and hence presumably of all minor constituents having their sources in the troposphere, in each hemisphere rises and falls with the seasons. This can be seen most clearly in figure 5, plate 2, where we show the deviation from the average for the year for each month. Local maxima relative to the mean occur at about 0.6 mbar and 20° latitude, towards the end of summer, i.e. in September–October in the Northern Hemisphere and March–April in the Southern (figure 5). Minima occur at the same latitudes six months later in each case. The predilection to associate regions of maximum abundance with places having the greatest vertical velocities is reinforced by noticing (figure 4, plate 1) that the late summer low-latitude maxima, in the Northern Hemisphere at least, are accompanied by higher-latitude minima, and vice versa. Unfortunately, the asymmetrical latitudinal coverage of SAMS does not permit us to say whether the Southern Hemisphere low-latitude maxima and minima are also accompanied by high-latitude extrema of the opposite sign. (The ISAMS, however, will provide coverage from 80°S to 80°N.) The 60° N minimum in CH_4 concentration could be produced by a mass of descending air, which has spent an extended period of time in the stratosphere and so become depleted of CH_4 by reaction with OH and other radicals. A single circulation cell with maximum upwelling at 20° and maximum downwelling at about 60° would then be implied. Because we are hypothesizing that the cells are solar driven, it is not surprising that the data show them building up in intensity during the summer and declining

Description of plate 2

Figure 5. Deviations from the three-years (1979–81 inclusive) annual mean mixing ratio of methane, expressed in percentages as a function of altitude (pressure) and season (month), for 10° latitude bins from 50° S to 70° N.

Figure 6. Deviations from the three-year (1979–81 inclusive) annual mean mixing ratio of methane, expressed in percentages as a function of latitude and season (month), on five constant pressure surfaces.

PHILOSOPHICAL TRANSACTIONS OF THE ROYAL SOCIETY A MATHEMATICAL, PHYSICAL & ENGINEERING SCIENCES

in the winter. The reversal of the abundance maxima and minima (figure 5) during late winter does not, of course, imply necessarily that the circulation reverses, since these are maxima and minima relative to the mean values at that particular latitude. In fact, the absolute amount of methane (and nitrous oxide) is always lower at 60° N than at 20° N (see figure 3, or table 2 of Taylor *et al.* 1986). Thus, in our interpretation of the observations, the sense of the circulation is always from equator to pole as we would expect, only its strength changing with the solar energy available to drive it.

Maps of the deviation from the mean as a function of time, plotted separately for each latitude band, appear in figure 4. These show that at any given latitude, the zonal mean abundance tends to peak earlier at higher altitudes, the opposite to the behaviour to be expected if material from the troposphere was simply being advected vertically. There has therefore to be strong horizontal, poleward, advection as well. The effect of this is greatest at about 0.6 mbar in mid-summer and gradually declines as the hemisphere moves towards winter. Thus, the picture emerges of a hemispherical Brewer–Dobson circulation growing in strength and vertical extent during the spring and declining after the summer solstice (figure 7).

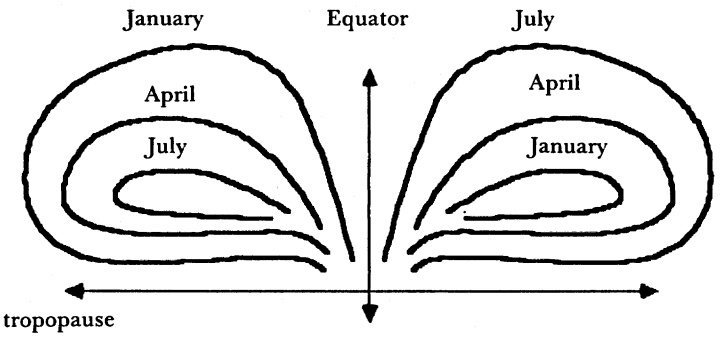

FIGURE 7. Schematic diagram of the general circulation of the stratosphere as deduced from the observations.

Not all aspects of the data are explained by this simple picture, however. At high altitudes (near the 0.5 mbar level) there is a pronounced semiannual oscillation (SAO) (figure 5) in the abundances of CH_4 and N_2O that, incidentally, is not present in the thermal structure when averaged in the same way. (The SAO in temperature at tropical latitudes is clearly seen in the SAMS data, but this has no corresponding detectable fluctuation in CH_4 abundance.) The methane SAO occurs at higher latitudes than the temperature SAO and is much more prominent in the Southern than the Northern Hemisphere.

There is also the 'double peaked' structure first remarked by Jones & Pyle (1984) that can be seen clearly in the April frame of figure 3. Gray & Pyle (1986) have interpreted this as being caused by downward velocities over the Equator that occur as a consequence of the SAO in tropical temperature and zonal wind. This is confirmed by Solomon *et al.* (1986) who calculated the transport from LIMS satellite observations of temperature.

Consider now the variations with latitude and season that take place on constant height (logarithmic pressure) surfaces (figure 6, plate 2), starting at the highest levels at which CH_4 was observed, i.e. 0.2 mbar or around 60 km. A non-seasonal trend is observed whereby all latitudes in both hemispheres tend to have maxima around September, and minima around March. This effect may be associated with the eccentricity of the Earth's orbit, and if so it

suggests that increased advection of ex-tropospheric air upwards because of stronger heating dominates increased photolytic destruction, as the solar intensity is greatest in the northern spring.

Lower down, the pattern described above with a low-latitude summer maximum and a high-latitude summer minimum emerges, until at about 35 km all latitudinal and seasonal variability becomes subdued. The reason for this is clear when lower levels are examined; the pattern reverses phase to give low-latitude summer minima and winter maxima in the 20 mbar (*ca.* 25 km) maps (figure 6). This we tentatively attribute to the returning branches of the hemispherical cells, depleted of minor constituent by photolysis during their long journey through the upper stratosphere, and re-entering the troposphere also at low latitudes (figure 7).

Conclusion

We have described one prominent category of instrument for middle-atmosphere measurements from satellites, and illustrated with one particular set of results from the SAMS, the mean distribution of methane as a function of season, how valuable these results can be for developing an understanding of the dynamical climatology of the region. Of course, our remarks do not constitute a full analysis of these data, even of the averages presented in the maps in figures 3–6. It is possible to use the measurements in calculations of the magnitudes of the sources and sinks of the species observed, and of the mean velocity fields. Work of this kind is going on, and Solomon *et al.* (1986) have shown, for example, that models of the CH_4 and N_2O fields computed by using transports from satellite temperature data agree quite well with the SAMS data. Holton (1986) has emphasized the importance of eddy transport in modifying the shape of the contours of constant mixing ratio produced by the diabatic circulation. Maps produced on a daily basis can provide additional insight, for example into features with a significant longitudinal dependence like those found in potential vorticity maps (Fairlie & O'Neill, this symposium; WMO 1986) or into rapid disturbances like those associated with stratospheric sudden warmings.

Although the SAMS and its sister experiments (like LIMS) broke new ground and their data will continue for some years to shed light on the problems of the middle atmosphere, there is of course plenty of scope for advancement. The biggest limitations of the SAMS data are their low vertical resolution, fairly limited signal to noise ratios, small selection of species (limiting the deductions about stratospheric photochemistry that are possible) and their incomplete latitude and solar longitude coverage. Great strides in all of these areas, and consequently in understanding the scientific problems, are expected with ISAMS and the *UARS* programme.

References

Barnett, J. J., Corney, M., Murphy, A. K., Jones, R. L., Rodgers, C. D., Taylor, F. W., Williamson, E. J. & Vyas, N. M. 1985 *Nature, Lond.* **313**, 439–443.

Drummond, J. R., Houghton, J. T., Peskett, G. D., Rodgers, C. D., Wale, M. J., Whitney, J. & Williamson, E. J. 1979 *Phil. Trans. R. Soc. Lond.* A **296**, 219–241.

Drummond, J. R. & Mutlow, C. T. 1981 *Nature, Lond.* **294**, 431–432.

Gray, L. G. & Pyle, J. A. 1986 *Q. Jl R. met. Soc.* **116**, 387–407.

Holton, J. R. 1986 *J. atmos. Sci.* **43**, 1238–1242.

Jones, R. L. & Pyle, J. A. 1984 *J. geophys. Res.* **89**, 5263–5279.

Jones, R. L. 1984 *Adv. Space Res.* **4**, 121–130.

Murphy, A. K. 1985 D. Phil. thesis, University of Oxford.

PHILOSOPHICAL TRANSACTIONS OF THE ROYAL SOCIETY A MATHEMATICAL, PHYSICAL & ENGINEERING SCIENCES

Rodgers, C. D., Barnett, J. J. & Jones, R. L. 1984 *J. geophys. Res.* **89**, 5280–5286.
Seeley, J. S., Hunniman, R. & Whatley, A. 1981 *Appl. Optics* **20**, 31–39.
Solomon, S., Kiehl, J. T., Garcia, R. C. & Grose, W. J. 1986 *J. atmos. Sci.* **43**, 1603–1617.
Taylor, F. W. 1983 *Spectrom. Techqs* **3**, 137–197.
Taylor, F. W. 1987 The physics of the climate problem. In *Science today* (ed. J. Mulvey). Oxford University Press.
Taylor, F. W., Dudhia, A. & Rodgers, C. D. 1986 *Adv. Space Res.* (In the press.)
Wayne, R. P. 1985 *Chemistry of atmospheres*. Oxford University Press.
WMO 1986 *Atmospheric ozone 1985*, World Meteorological Organization report no. 16, ch. 6. Geneva: WMO.

The colour plates in this paper were printed by George Over Limited.

PHILOSOPHICAL TRANSACTIONS OF THE ROYAL SOCIETY A MATHEMATICAL, PHYSICAL & ENGINEERING SCIENCES

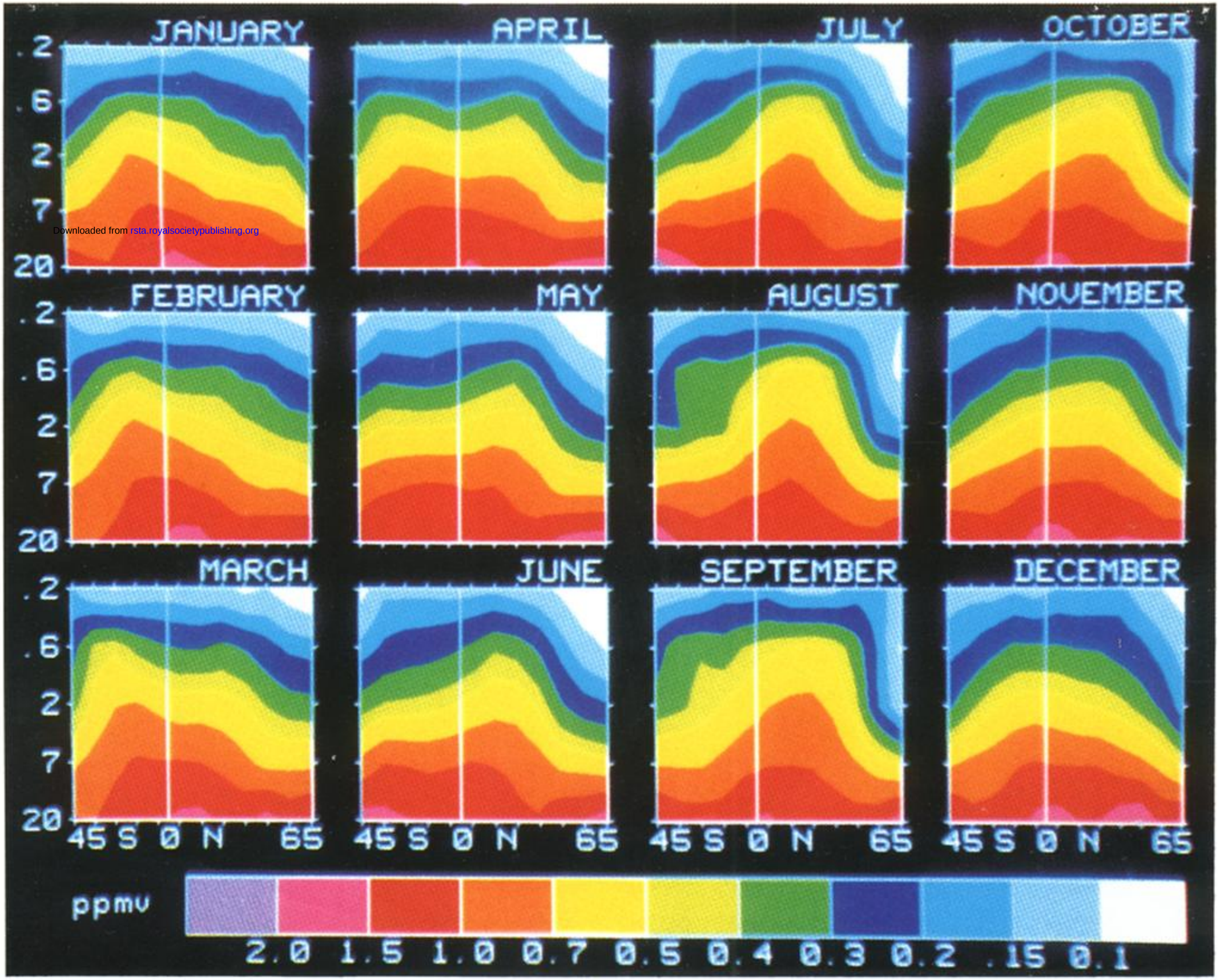

FIGURE 3. Monthly mean abundances of methane in parts per million by volume as measured by SAMS. The ordinate is logarithmic pressure from 20 to 0.2 mbar (approximately 20–60 km), and the abscissa is latitude. The data are zonal averages in 10° latitude bins for the three years 1979–81.

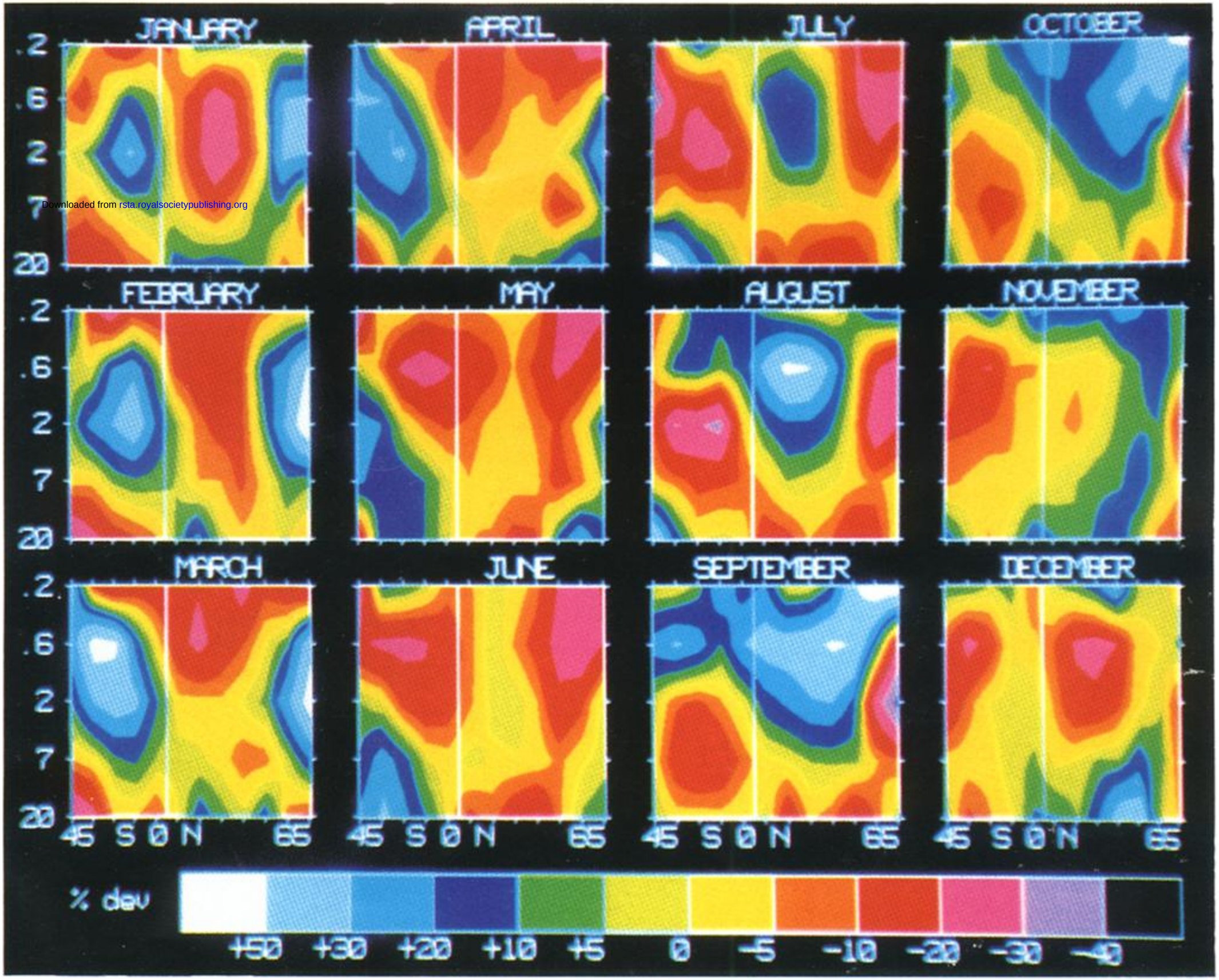

FIGURE 4. Deviations from the three-year (1979–81 inclusive) annual mean mixing ratio of methane, expressed in percentages as a function of altitude (pressure) and latitude, for each month of the year.

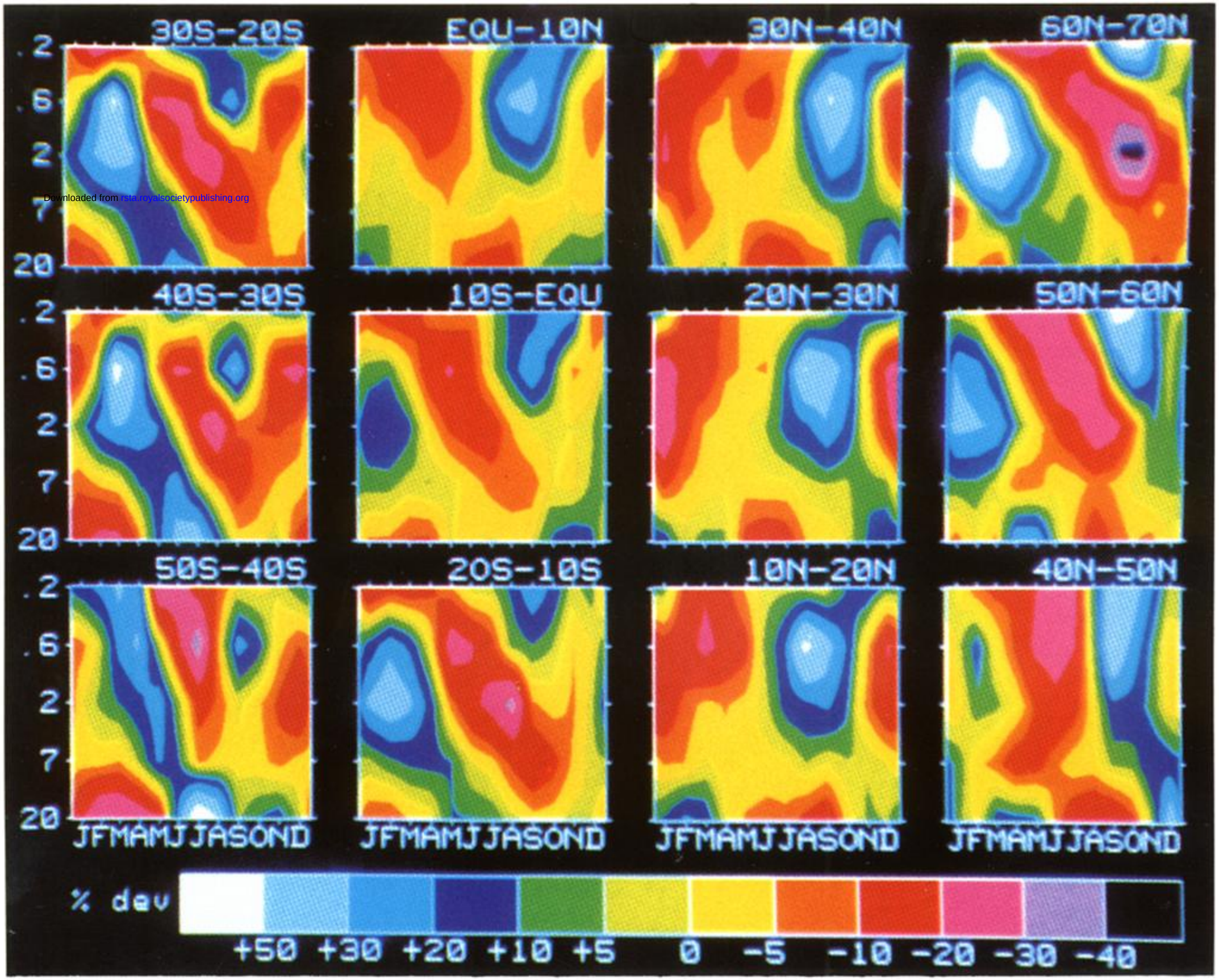

GURE 5. Deviations from the three-years (1979–81 inclusive) annual mean mixing ratio of methane, expressed in percentages as a function of altitude (pressure) and season (month), for 10° latitude bins from 50° S to 70° N.

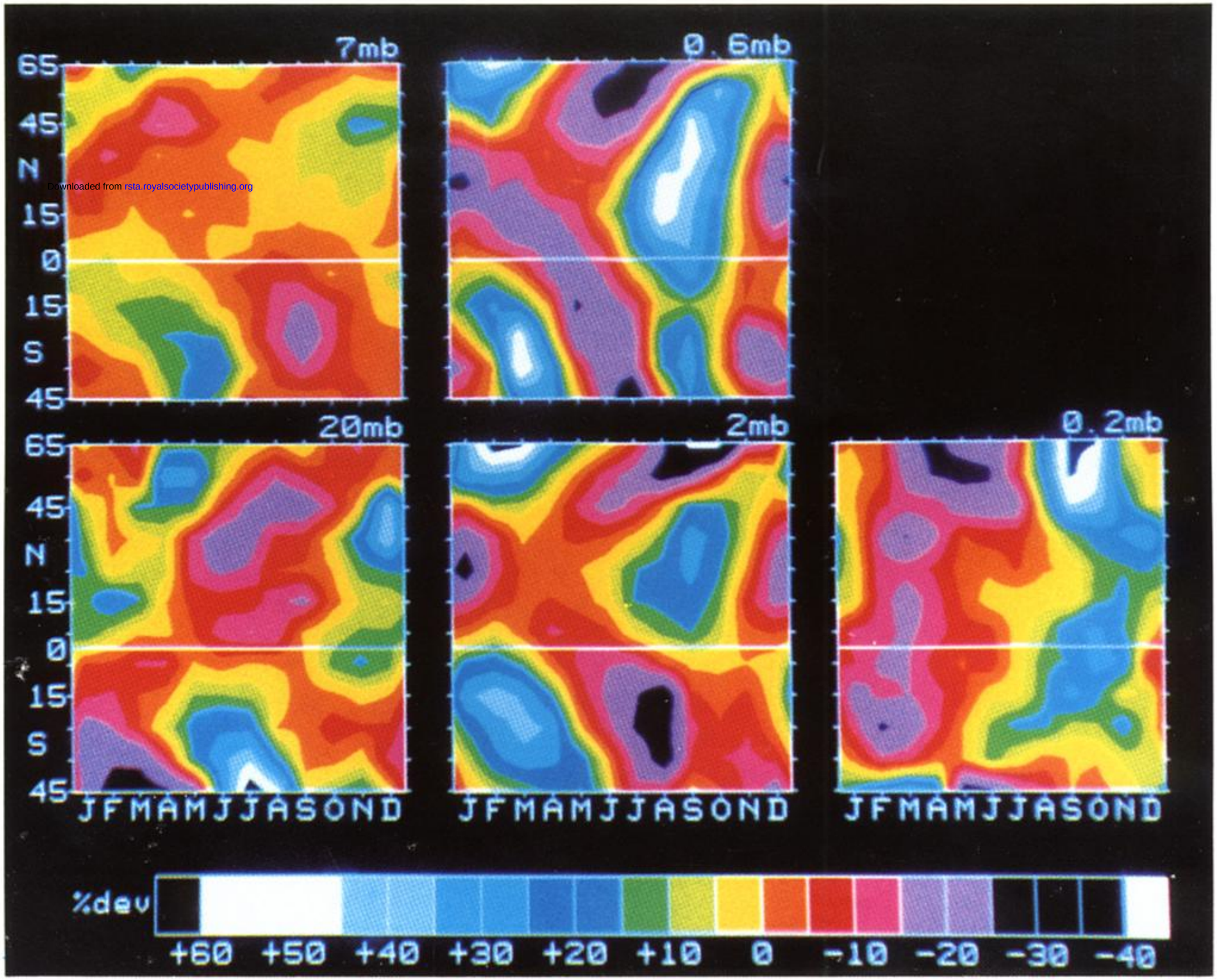

GURE 6. Deviations from the three-year (1979–81 inclusive) annual mean mixing ratio of methane, expressed in percentages as a function of latitude and season (month), on five constant pressure surfaces.